High pressure compressibilities of pyrite and cattierite

Tetsuo FUJII*, Akira YOSHIDA*, Kiyoaki TANAKA*, Fumiyuki MARUMO*
and Yasutoshi NODA**

*Research Laboratory of Engineering Materials, Tokyo Institute of Technology, Nagatsuta 4259, Midori, 227 Yokohama, Japan
**Department of Materials Science, Faculty of Technology, Tohoku University, Aoba, 980 Sendai, Japan

Abstract

Compressibilities of pyrite and cattierite have been examined by the single-crystal X-ray diffraction method up to 42 kbar and 36 kbar, respectively. Both S-S and M-S (M: Fe, Co) bonds in both of the minerals are contracted linearly with pressure within the experimental pressure ranges. However, contraction of the S-S bond in cattierite is much smaller than that in pyrite, whereas the Co-S bond shows a larger contraction than Fe-S. Bonding strength (or hardness) of the S-S bond is estimated to be about 60% of that for Fe-S in pyrite.

Introduction

Although pyrite (FeS_2) and cattierite (CoS_2) have the same type of structure (pyrite type), they show fairly different electric properties with each other. The former is a semi-conductor, whereas the latter shows a metallic conductivity. Since the difference should originate from the characters of their chemical bonds, it is expected for these two crystals to show difference in their compressibilities.

Will et al. (1984) reported that the S-S bond distances of pyrite and cattierite increased under high pressure up to 40 kbar by X-ray diffraction. On the other hand, examinations of these compounds by Raman spectroscopy (Takahashi et al., 1985) indicated a contraction of the S-S distance in pyrite and retention of the distance in cattierite under high pressure. Examination of pyrite by EXAFS spectroscopy (Ingalls et al., 1978) also indicated the contraction of the S-S bond distance in pyrite under high pressure. The results of Raman and EXAFS spectroscopies contradict those of X-ray analysis.

The present authors intended to settle the problem by applying the single-crystal diffraction technique under hydrostatic high-pressure with the aid of diamond-anvil cells.

Experimental

Pyrite

The diamond-anvil cell designed by Miyake *et al.* (1982) was used for the high-pressure diffraction experiments. The diamond crystals of the cell were 1/6 carat each, 0.6 mm in culet diameter, 3.3 mm in table diameter and 1.4 mm in height. The gasket with the thickness of 0.3 mm was made of SUS631 stainless steel.

A crystal of natural pyrite from Kanehorizawa mine at Aomori city in Japan was crashed into pieces, and a platy fragment (0.15×0.10×0.05 mm) was selected out for the diffraction experiments. Before it was set into the diamond-anvil cell, X-ray diffraction intensity data were collected under the ambient condition with MoKα radiation monochromatized with pyrolytic graphite. The measurements were carried out on a four-circle diffractometer (Rigaku AFC-5UD) in the range $2\theta \leq 90°$ with the 2θ-ω scan technique, and gave 561 reflection data satisfying the condition of $|F_0| \geq 3\sigma (|F_0|)$. The number of crystallographically independent reflections was 202.

After the above measurements, the specimen was put into the hole (0.3 mm in diameter) of the gasket together with a piece of ruby crystal for pressure calibration (Piermarini *et al.*, 1975), and stuck on a culet face of a diamond crystal by grease. Then the hole of the gasket was filled with a pressure transmitting medium of 4:1 methanol-ethanol mixture (Piermarini *et al.*, 1973; Finger & King, 1978).

Cell dimensions under the respective pressure were determined from 2θ values of 25 reflections in the ranges of $55° < 2\theta < 80°$ for MoKα and $36° < 2\theta < 44°$ for AgKα

TABLE 1. Crystal data of pyrite and cattierite. Results of cattierite at 1 bar are quoted from those reported by Noda and Sato (1983).

	FeS_2	CoS_2
Space group	Pa3	Pa3
Cell dimension a (Å)		
1 bar	5.4170(1)	5.5348(4)
19 kbar	—	5.5068(3)
31 kbar	5.3825(5)	—
36 kbar	—	5.4799(4)
42 kbar	5.3702(5)	—
Z	4	4
ρ_{calc} at 1 bar (g/cm³)	5.014	4.821
μ at 1 bar (cm⁻¹)		
λ: MoKα	115.4	122.1
λ: AgKα	59.1	62.5

radiation by the least-squares method. The obtained values are given in Table 1. The space group Pa3 was confirmed from the Laue symmetry and the extinction rules of reflections.

Diffraction intensity measurements were carried out on the Rigaku automated four-circle diffractometer at room temperature under 31 and 42 kbar. $AgK\alpha$ radiation monochromatized with pyrolytic graphite was used for the measurements in place of $MoK\alpha$ radiation to increase the accessible area of reciprocal space. A slow scan speed (one half of that in the measurement using $MoK\alpha$ radiation) was adopted to compensate the weak diffraction intensities of $AgK\alpha$ radiation. Centering of the crystal was performed with King and Finger's method, in which four-circle axial angles of eight equivalent reflections were refined. Deviations in the position of the crystal from the center of the goniostat were calculated from the observed angles for diffracted radiation (King & Finger, 1979). After the orientation of the crystal was determined, the holes of hemispherical beryllium windows (Miyake et al., 1982) were filled with beryllium rods, so that the beryllium windows might form perfect hemispheres and give equal absorption effects for all reflections.

Intensity data were collected in the fixed ϕ mode. Reflections in the region of $2\theta \leq 90°$ can be measured, since the open angle of the window of the cell is $90°$. However, it was found that several reflections at the higher angles were hidden by the gasket or by the steel base of the cell, even when the 2θ angles were lower than $90°$. Therefore, the maximum 2θ angles were set at $80°$ and $70°$ in the measurements under 42 and 31 kbar, respectively. The ω-scan was adopted in the region of $0° < 2\theta \leq 40°$, whereas the 2θ-ω scan was employed in the higher angle region. For all reflections, peak profiles were recorded to check overlapping of reflections from diamond or beryllium, and shadowing by the steel base of the high-pressure device.

Background counts were primarily caused by the scattering from beryllium windows. Since most of strong powder lines of metallic beryllium were present in the region of $2\theta \leq 40°$ for $AgK\alpha$ radiation, the ω-scan mode was adopted in this region. The powder lines of beryllium would not disturb reflections from the specimen, if the intensities are measured in the ω-scan mode. However, it was revealed that several reflections were perturbed by beryllium powder lines in the higher angle region. These reflections could be discriminated from the data set with referring to their 2θ angles and the diffraction profile. Those overlapped with diamond reflections were also deleted.

The reflections partially shadowed by the edge of steel base give a significantly low background at the higher angle side of ω, and can be easily recognized from their peak profiles. On the other hand, those by the gasket reduce both their background and peak intensities, and can be noticed through comparison of the intensity with those of equivalent reflections. The values of α_p (the angle between the incident beam

and the radial symmetry axis of the diamond-anvil cell) and α_d (the angle between the diffracted beam and the radial symmetry axis of the cell) are also helpful to recognize the interference by the gasket (Fujii & Marumo, 1986). It should be noticed that the critical values of α_p and α_d depend on the χ angle, when the specimen is not at the center of the gasket hole. The reflections which were cut by the edge of steel base or by the gasket were deleted from the data set.

The observed intensities were corrected for the Lorentz, polarization and absoption factors. Since absorption effect caused by the beryllium windows was identical for all reflections in the present case, no corrections were made for this effect. The absorptions due to the diamond crystals were corrected after the method reported by Finger & King (1978). Finally, 481 and 576 reflection data with $|F_0| \geq 3\sigma(|F_0|)$ were obtained in the measurements under 31 and 42 kbar, respectively, and used for structure refinements. Here, $\sigma(|F_0|)$ is the standard deviation of the observed structure amplitude $|F_0|$ based on the counting statistics. The numbers of crystallographically independent reflections were 92 and 115, respectively.

Cattierite

Powder of cattierite (CoS_2) was synthesized by direct reaction of metallic cobalt and sulfur at $600^\circ C$. Crystals were grown from this powder with a chemical transport method. A single crystal with dimensions $0.14 \times 0.10 \times 0.06$ mm was selected out for X-ray diffraction experiments. Intensities were measured under 19 and 36 kbar at room temperature with the aid of the diamond-anvil cell in a similar way to that employed in the measurement on pyrite. The measurements were carried out with $AgK\alpha$ radiation. The maximum 2θ angle was set at 75°, and the ω scan technique was adopted in all the 2θ range. The observed intensities were corrected for the Lorentz, polarization and absorption factors. The cell dimensions under the respective pressures were determined from 2θ values of the set of 25 reflections in the range $35^\circ < 2\theta < 43^\circ$ by least-squares calculations. The 709 and 721 reflection data with $|F_0| \geq 3\sigma(|F_0|)$ were used for refinements of structures under 19 and 36 kbar, respectively. Crystallographically independent reflections in these data sets were 128 and 137.

Structure refinements

In all the structure refinements, equivalent reflections were not averaged, and treated as independent reflection data. The structure parameters of pyrite under room pressure were refined by a full-matrix least-squares program LINKT85, starting from the atomic parameters given by Elliott (1960). Structure refinements of pyrite and cattierite under high pressures were carried out with the same program, starting from

TABLE 2. The final atomic parameters of pyrite and cattierite at 1bar and under high pressures. The temperature factors are the coefficients in the expression exp $[-(2\pi^2/a^2)$ $\{U_{11}(h^2+k^2+l^2)+2U_{12}(kl+lh+hk)\}$]. Results of cattierite at 1bar are quoted from those reported by Noda and Sato (1983).

	FeS$_2$			CoS$_2$		
	1bar	31kbar	42kbar	1bar	19kbar	36kbar
x	0.3848(1)	0.3849(1)	0.3849(1)	0.38989(1)	0.3896(1)	0.3890(1)
U_{11}(M)	0.0036(2)	0.0079(2)	0.0036(1)	0.00446(2)	0.0052(1)	0.0049(1)
U_{12}(M)	−0.0001(1)	0.0004(3)	0.0003(2)	−0.00010(2)	−0.0002(1)	0.0000(2)
U_{11}(S)	0.0042(2)	0.0090(1)	0.0044(2)	0.00464(2)	0.0054(1)	0.0052(1)
U_{12}(S)	0.0000(2)	0.0004(3)	0.0002(2)	−0.00016(3)	−0.0002(2)	−0.0001(2)

M: (0,0,0), S: (x,x,x)

$U_{11}=U_{22}=U_{33}$ and $U_{12}=U_{23}=U_{13}$ for both M and S

the final atomic parameters of pyrite under room pressure. In the first cycle of refinements, only a scale factor was varied, and then one positional parameter of S, anisotropic temperature factors of metal and S, and anisotropic secondary extinction correction parameters (Becker & Coppens, 1974) were varied together with the scale factor. The final weighted discrepancy factors R_w were about 0.040 for pyrite under all of the three experimental pressures, 0.045 and 0.049 for cattierite under 19 and 36 kbar, respectively. The value of $\Sigma(|F_0|-k|F_0|)^2$ was minimized. Atomic scattering factors for neutral atoms and anomalous dispersion factors were taken from International Tables for X-ray Crystallography (1974). The final atomic parameters are given in Table 2.

TABLE 3. The bond distances (Å) and bond angles (°) in pyrite and cattierite at 1bar and under high pressures. Results of cattierite at 1bar are quoted from those reported by Noda and Sato (1983).

		S-S	M-S	S-M-S	M-S-S	M-S-M
	1bar	2.162(1)	2.2636(4)	94.36(2) & 85.64(2)	102.32(2)	115.58(2)
FeS$_2$	31kbar	2.146(1)	2.249(1)	94.35(2) & 85.65(2)	102.34(3)	115.56(3)
	42kbar	2.141(1)	2.244(1)	94.35(2) & 85.65(2)	102.34(3)	115.56(3)
	1bar	2.111(1)	2.3237(1)	93.94(1) & 86.06(1)	103.49(1)	114.73(1)
CoS$_2$	19kbar	2.107(1)	2.311(1)	93.97(2) & 86.03(2)	103.42(3)	114.78(2)
	36kbar	2.107(1)	2.299(1)	94.01(2) & 85.99(2)	103.30(3)	114.88(2)

Results and discussion

In the pyrite-type structures, metal atoms locate at (0,0,0), and sulphur atoms at (x,x,x) in the space group Pa3. Two sulphur atoms at (x,x,x) and $(1-x,1-x,1-x)$ are considered to form an S_2 molecule with a fairly short distance of about 2.1 Å. Therefore, a structure of this type is characterized by the cell dimension and the S-S bond distance.

The interatomic distances and bond angles in pyrite and cattierite are given in Table 3. The values of pyrite under room pressure are in an excellent agreement with those reported by Stevens *et al.* (1980). The transition metal atoms have trigonally deformed octahedral coordinations with S atoms. Each S atom is tetrahedrally coordinated with three metal and one sulphur atom. The cell dimensions of the two crystals are plotted against pressure in Fig. 1. The pressure dependence of the individual bond lengths are shown in Fig. 2 and Fig. 3 for pyrite and cattierite, respectively. Both cell dimension and bond distances show exactly linear relations to pressure in either of the crystals. The value of a-dimension (Å) is related to the pressure (kbar) with the following formulae,

$$a=5.4181-0.00115P \qquad\qquad (1)$$

for pyrite and,

$$a=5.5364-0.00156P \qquad\qquad (2)$$
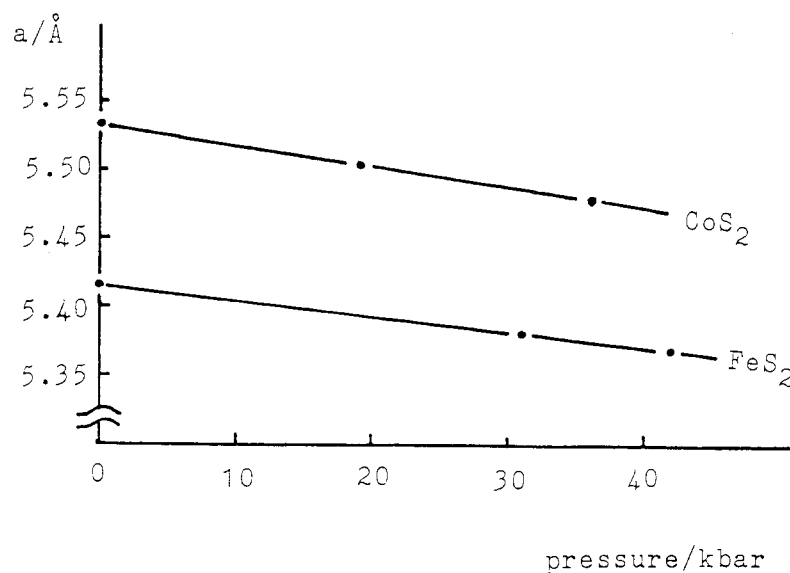

FIG. 1.   Pressure dependence of cell dimensions of pyrite and cattierite.
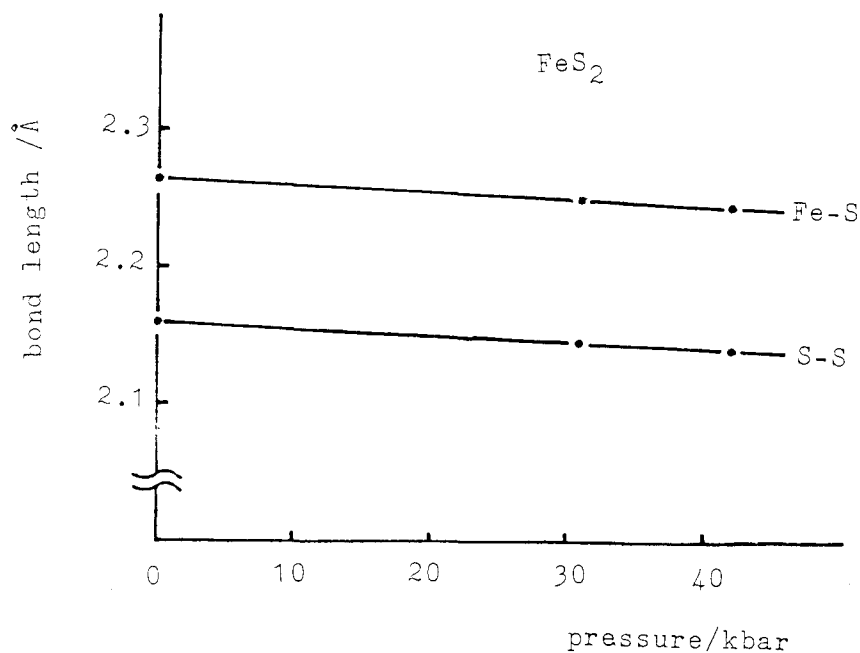
FIG. 2.   Pressure dependence of bond lengths in pyrite.

for cattierite.

Contrary to the results reported by Will *et al.* (1984), both S-S and Fe-S bonds contract with increasing pressure in accordance with Raman spectroscopy and EXAFS measurements. The linear relation between the bond length and pressure indicates that the two-body potential along the bond is harmonic in a good approximation within the pressure range of this experiment. The slope of the bond length—pressure plots gives an estimate of strength of the bond for stress (or hardness of the bond). If F is the interatomic force between the relevant atoms and Δl the difference of bond length from the value l under the atmospheric pressure, the following relation holds with the harmonic approximation,

$$F = -k \cdot \Delta l / l, \qquad\qquad (3)$$

where k is a force constant.

When the values for S-S and Fe-S bonds in pyrite are represented with the subscripts 1 and 2, respectively, equilibrium of forces on sulphur atom along the direction of the S-S bond (Fig. 4) requires the following relation,

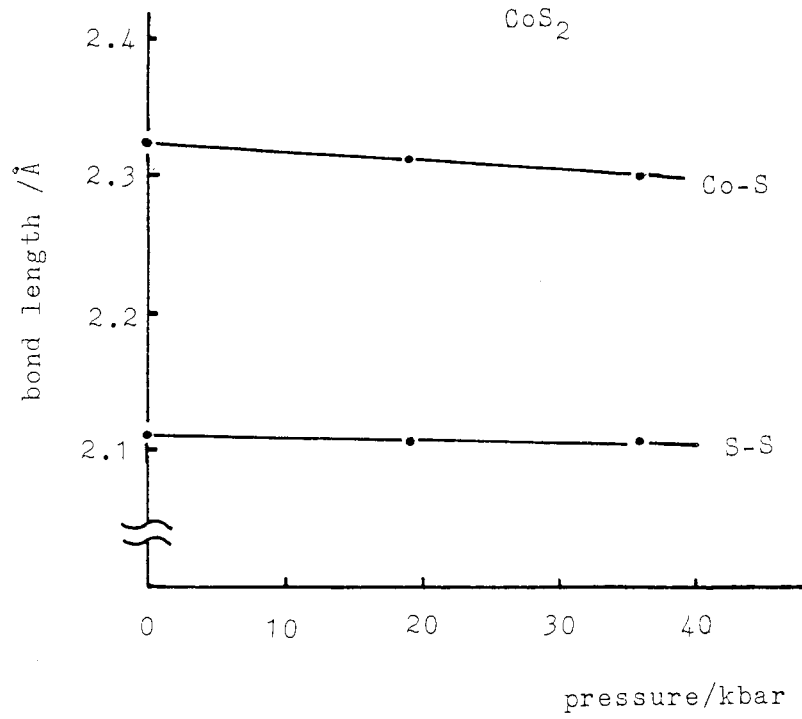$$F_1 = 3F_2 \sin\xi, \qquad\qquad (4)$$

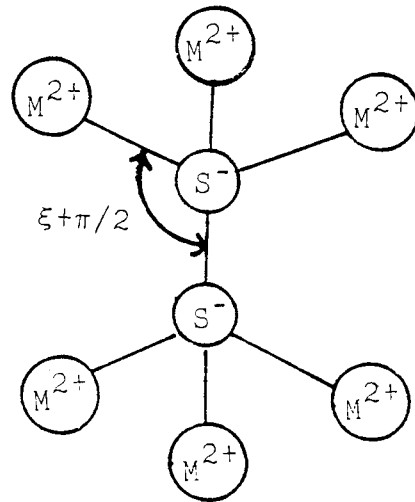FIG. 3.   Pressure dependence of bond lengths in cattierite.

FIG. 4.   Configuration of cations around the S_2^{2-} group in the pyrite-type crystals.

where $\xi + \pi/2$ is the angle between the Fe-S and S-S bonds. Substituting the equation (4) for (3) we obtain,

$$k_1 \Delta l_1 / l_1 = 3 k_2 (\Delta l_2 / l_2) \sin \xi. \qquad (5)$$

Table 3 gives the following values for l, Δl and ξ:

$l_1 = 2.1615(5)$ Å, $l_2 = 2.2636(4)$ Å,

$\Delta l_1 (31 \text{ kbar}) = -0.016(1)$ Å, $\Delta l_2 (31 \text{ kbar}) = -0.015(1)$ Å, $\xi (31 \text{ kbar}) = 12.34(3)°$,

$\Delta l_1 (42 \text{ kbar}) = -0.021(1)$ Å, $\Delta l_2 (42 \text{ kbar}) = -0.020(1)$ Å, $\xi (42 \text{ kbar}) = 12.34(3)°$,

Substituting these values into the equation (5), we obtain the ratio of the bonding strength (or hardness) of the S-S and Fe-S bonds:

$$k_1 / k_2 = 0.59(3) \text{ at } 31 \text{ kbar},$$

and

$$k_1 / k_2 = 0.60(3) \text{ at } 42 \text{ kbar}.$$

Namely the bonding strength of the S-S bond is about 60% of that of Fe-S bond.

If we denote the cell volume and pressure with V and P, respectively, compressibility is given with $-\dfrac{1}{V} \dfrac{\partial V}{\partial P}$. Since V is equal to a^3, and a is related to P with the equation (1) or (2), we can express the compressibilities of the two crystals with P. Namely, the compressibilities are

$0.00345/(5.4181 - 0.00115P)$ for pyrite,

and $0.00468/(5.5364 - 0.00156P)$ for cattierite.

As seen from Figs. 2 and 3, contraction of the S-S bond in cattierite under high pressure is very small compared with that in pyrite, whereas the Co-S bond shows a larger contraction than the Fe-S bond under high pressure. These facts accord with the shorter S-S and the longer M-S bond lengths at room pressure in cattierite than in pyrite.

Fig. 4 shows the configuration of cations around the $S_2{}^{2-}$ group in the pyrite-type compound. Two S^- ions are joined each other by a σ bond. The S-S bond distances are 2.06 Å both in S_6 and S_8 molecules, where S atoms are bound by σ bonding, and shorter than the S-S distances in pyrite and cattierite. The lengthening of S-S distances in pyrite-type crystals is supposed to be caused by electrostatic forces between ions in these crystals. Namely, cations surrounding the $S_2{}^{2-}$ group pull the group from both sides of the group by the electrostatic attractive forces, and the two S^- anions repel each other. Thus, the $S_2{}^{2-}$ groups in pyrite and cattierite are expected to give longer S-S distances than those in the S_6 and S_8 molecules.

Transition metals have the low-spin configurations in pyrite-type crystals as indicated by the magnetic susceptibilities (Burns, 1970). On the basis of the crystal

field theory, in the low-spin state, a Co^{2+} ion in an octahedral field has one electron in the dγ orbitals, while an Fe^{2+} ion has no electron in these orbitals. In cattierite, the repulsion between this electron in dγ and the p-electrons of the ligands weakens the electrostatic attraction between the S^- anion and Co^{2+} cation, giving the longer M-S distance at room pressure. The elongated M-S bond brings the shorter distance of the S-S bond. Since the electronic configurations of S_2^{2-} groups in cattierite and in pyrite are identical within the approximation of the crystal field theory, a smaller contraction of the S-S bond with pressure is expected in cattierite than in pyrite because of the shorter S-S distance in cattierite at room pressure.

References

BECKER, P. J. & COPPENS, P. (1974) *Acta Cryst.*, **A30**, 129-147.
BURNS, R. G. (1970) *Mineralogical Applications of Crystal Field Theory*, p. 192, Cambridge University Press, London.
BUSING, W. R. & LEVY, H. A. (1957) *Acta Cryst.*, **10**, 180-182.
ELLIOTT, N. (1960) *Journ. Chem. Phys.*, **33**, 903-905.
FINGER, L. W. & KING, H. (1978) *Amer. Miner.*, **63**, 337-342.
FUJII, T. & MARUMO, F. (1986) *Miner. Journ.*, **13**, 111-118.
INGALLS, R., GARCIA, G. A. & STERN, E. A. (1978) *Phys. Rev. Lett.*, **40**, 334-336.
International Tables for X-ray Crystallography, IV (1974) The Kynoch Press, Birmingham.
KING, H. & FINGER, L. W. (1979) *Journ. Appl. Cryst.*, **12**, 374-378.
MERRILL, L. & BASSET, W. A. (1974) *Rev. Sci. Instrum.*, **45**, 290-294.
MIYAKE, M., FUJII, T, ISHII, H. & MARUMO, F. (1982) *Report RLEMTIT*, **7**, 1-7.
NODA, Y. & SATO, S. (1983) *Abstr. the 38'th Annual Meeting of the Phys. Soc. of Japan.*, p. 164.
PIERMARINI, G. J., BLOCK, S. & BARNETT, J. D. (1973) *Journ. Appl. Phys.*, **44**, 5377-5382.
PIERMARINI, G. J., BLOCK, S., BARNETT, J. D. & FORMAN, R. A. (1975) *Journ. Appl. Phys.*, **46**, 2774-2780.
STEVENS, E. D., DELUCIA, M. L. & COPPENS, P. (1980) *Inorg. Chem.*, **19**, 813-820.
TAKAHASHI, H., MINOMURA, S. & MŌRI, N. (1985) *Abstr. the 26'th High Pressure Conference of Japan*, pp. 20-21.
WILL, G., LAUTERJUNG, J., SCHMITZ, H. & HINZE, E. (1984) *Mat. Res. Soc. Symp. Proc.*, **22**, 49-52.